



A Static and Free Vibration Analysis of Porous Functionally Graded Beams

Lazreg Hadji

Department of Civil Engineering, University of Tiaret, Tiaret, Algeria
lazreg.hadji@univ-tiaret.dz

Vagelis Plevris

Department of Civil and Architectural Engineering, Qatar University, Doha, Qatar
vplevris@qu.edu.qa

Royal Madan

Department of Mechanical Engineering, G H Raisoni Institute of Engineering and Technology, Nagpur, India
royalmadan6293@gmail.com

Abstract

In this work, the static and free vibration analysis of functionally graded (FG) porous beams is investigated using a new higher-order shear deformation model (HSD). The porosity that develops naturally during the fabrication of a material is arbitrary in nature. Therefore, in the present study, a variation is considered taking into account three distribution patterns, namely (i) even distribution, (ii) uneven distribution, and (iii) the logarithmic-uneven pattern. Furthermore, the impact of several micromechanical models on the bending and free vibration behavior of the beams was investigated. Different micromechanical models were used to examine the mechanical properties of functionally graded beams, the properties of which change continuously throughout the thickness following a power law. Using the HSD model, the equations of motion are obtained using Hamilton's principle. To obtain displacements, stresses, and frequencies, the Navier type solution method was employed, and the numerical results were compared to those published in the literature. The impact of porosity and volume fraction index, different micromechanical models, mode numbers, and geometry on the bending and natural frequencies of imperfect FG beams were investigated.

Keywords: FG beam; Bending; Free vibration; Functionally graded materials; Porosity

1 Introduction

Functionally graded materials (FGMs) are special materials whose properties change along the length/thickness because of a change in the composition of two materials' porosity, and microstructure (Avcar, 2019; Hadji & Avcar, 2021; Sankar, 2001). A functionally graded material has varied thermo-mechanical properties and as a result, the yield strength of FGMs will vary. The effect of porosity on the limit speed analysis of a rotating disk was studied using variational principles under different loads, such as rotation and thermal (Madan & Bhowmick, 2021). The detailed dynamic analysis of a beam can pose significant computational challenges (Plevris & Tsiatas, 2018). In this work, the dynamic analysis was performed using finite element analysis, shear deformation theory, and modified shear deformation theory (Benaberrahmane et al., 2021; Larbi et al., 2013; Nguyen et al., 2017; Şimşek, 2010; Thai & Vo, 2012). The present study investigates the effect of porosity and volume fraction index, different micromechanical models, and geometry on the bending and natural frequencies of imperfect functionally graded (FG) beams. The power law variation of composition was considered to grade the beam in the transverse direction. Different material models were used to model the effective material properties of the FG beam. Hamilton's principle was used

in combination with Navier’s method. The natural frequency of FG beams was calculated for different grading indices for both the longitudinal and the thickness directions. The analysis of imperfections in FGM beams reveals a logarithmic uneven distribution compared to other imperfection types studied. An even porosity distribution must be avoided and accordingly the proper manufacturing process has to be selected.

2 Effective Properties of FGMS

Fig. 1 shows the different models that are used to estimate the material properties effectively. The different models used are Voigt, Reuss, Tamura, local representative volume element (LRVE), and Mori-Tanaka model. Voigt and Reuss assume perfect bonding between fibers, so when the reinforcement is of particulate type and not long fibers, then Voigt and Reuss do not give good results. In such cases, the Tamura model (an empirical model) can be used. In this model, the term q is the stress-strain transfer ratio that can be calculated experimentally and numerically. A detailed description of all these models for different material properties and their estimates for different material combinations can be found in (Madan & Bhowmick, 2022).

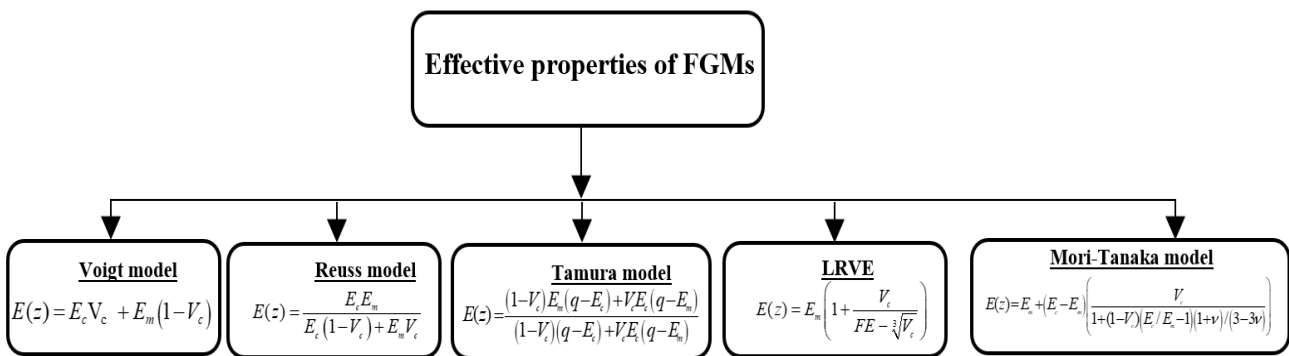


Fig. 1: Different material modeling methods

3 Preliminary Concepts and Definitions

We consider an FG beam of length L and cross section $b \times h$, as shown in Fig. 2(a). The gradation of the beam is changing along the thickness direction.

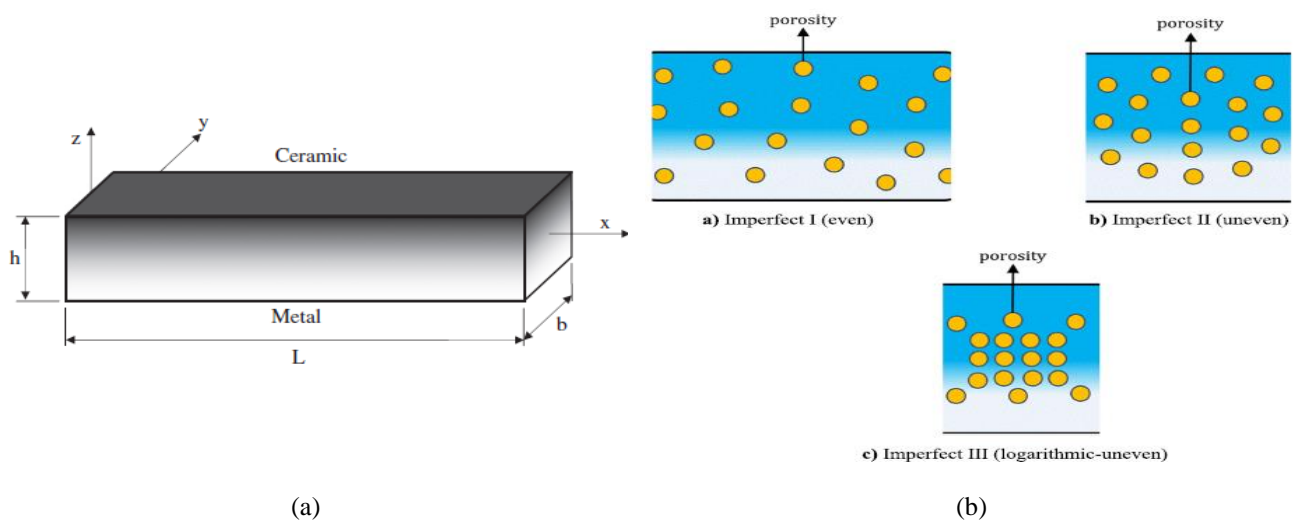


Fig. 2: (a) Geometry and coordinate system of an FG beam, (b) Porosity models

A beam is made of FGMs of which the volume fraction variation of ceramic and metal are denoted as $V_c(z)$ and $V_m(z)$, respectively, and are given by the formulas:

$$V_c(z) = \left(\frac{z}{h} + \frac{1}{2} \right)^p \quad (1)$$

$$V_m(z) = 1 - V_c(z) \quad (2)$$

Where, p is the volume fraction index that defines how the combination of metal and ceramic is distributed, with $0 \leq p \leq \infty$. For $p = 0$, the beam is purely made of ceramic, whereas for $p = \infty$, it is purely metal.

3.1 Porosity-dependent Functionally Graded Materials

The characteristic of materials of FG porous beams can be written as

$$P(z) = (P_c - P_m) \left(\frac{z}{h} + \frac{1}{2} \right)^p + P_m - P_{por} \quad (3)$$

In this study, three types of porosity are considered; the first of them presents an even distribution (called hereafter Imperfect I), whereas the other ones are characterized by an uneven distribution (Imperfect II and III hereafter), along the beam thickness direction, as shown in Fig. 2(b). The various expressions of the porosity distribution are presented in detail in Table 1.

Table 1: Porosity Distribution Types

Imperfect I	Imperfect II	Imperfect III
$P_{por} = \frac{\alpha}{2} (P_c + P_m)$ <p style="text-align: center;">(4)</p>	$P_{por} = \frac{\alpha}{2} \left(1 - \frac{2 z }{h} \right) (P_c + P_m)$ <p style="text-align: center;">(5)</p>	$P_{por} = \log \left(1 + \frac{\alpha}{2} \right) \left(1 - \frac{2 z }{h} \right) (P_c + P_m)$ <p style="text-align: center;">(6)</p>
$\begin{bmatrix} E(z) \\ \beta(z) \\ \rho(z) \end{bmatrix} = \begin{bmatrix} E_{cm} \\ \beta_{cm} \\ \rho_{cm} \end{bmatrix} \left(\frac{z}{h} + \frac{1}{2} \right)^p + \begin{bmatrix} E_m \\ \beta_m \\ \rho_m \end{bmatrix} - \frac{\alpha}{2} \begin{bmatrix} E_c + E_m \\ \beta_c + \beta_m \\ \rho_c + \rho_m \end{bmatrix}$ <p style="text-align: center;">(7)</p>	$\begin{bmatrix} E(z) \\ \beta(z) \\ \rho(z) \end{bmatrix} = \begin{bmatrix} E_{cm} \\ \beta_{cm} \\ \rho_{cm} \end{bmatrix} \left(\frac{z}{h} + \frac{1}{2} \right)^p + \begin{bmatrix} E_m \\ \beta_m \\ \rho_m \end{bmatrix} - \frac{\alpha}{2} \left(1 - \frac{2 z }{h} \right) \begin{bmatrix} E_c + E_m \\ \beta_c + \beta_m \\ \rho_c + \rho_m \end{bmatrix}$ <p style="text-align: center;">(8)</p>	$\begin{bmatrix} E(z) \\ \beta(z) \\ \rho(z) \end{bmatrix} = \begin{bmatrix} E_{cm} \\ \beta_{cm} \\ \rho_{cm} \end{bmatrix} \left(\frac{z}{h} + \frac{1}{2} \right)^p + \begin{bmatrix} E_m \\ \beta_m \\ \rho_m \end{bmatrix} - \log \left(1 + \frac{\alpha}{2} \right) \begin{bmatrix} E_c + E_m \\ \beta_c + \beta_m \\ \rho_c + \rho_m \end{bmatrix}$ <p style="text-align: center;">(9)</p>

For the various porosity distribution models, the material parameters of FG porous beam, such as the elastic modulus E , the thermal expansion coefficient β , and mass density ρ , were then calculated by employing the rule of mixture.

3.2 Equations of Motion

The Hamilton's principle was employed, for which the strain energy (U) and kinetic energy (K) relations are shown in Fig. 3. A detailed solution algorithm is not included here, to maintain the brevity of the manuscript. For details on the solution algorithm, the interested reader is referred to the work of (Avcar, 2019).

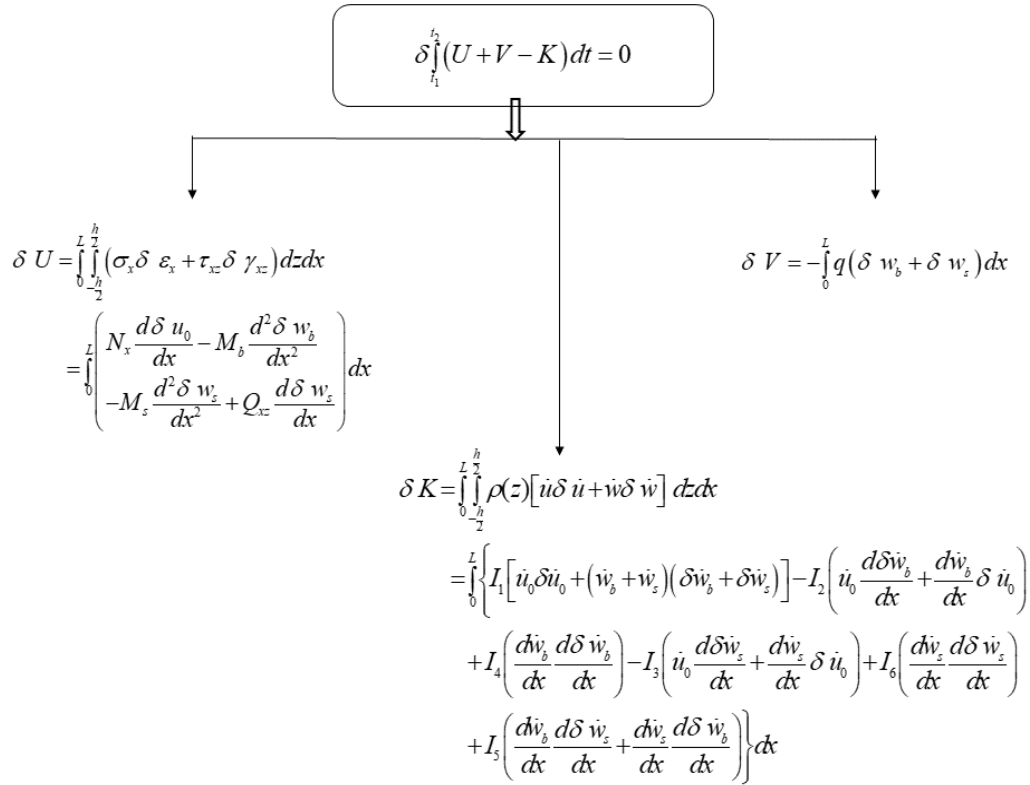


Fig. 3: Solution Methodology

4 Results and Discussion

The validation study of the bending and free vibration responses of simply supported porous FG beams was performed with comparison to published results. To perform the analytical calculations of this work we used the Maple software. The beam material selected has the following characteristics:

- Ceramic (P_c : Alumina, Al_2O_3): $E_c = 380$ GPa; $\nu = 0.3$; $\rho_c = 3960$ kg/m³.
- Metal (P_m : Aluminium, Al): $E_m = 70$ GPa; $\nu = 0.3$; $\rho_m = 2702$ kg/m³.

For convenience, the following dimensionless forms are used:

$$\bar{w} = 100 \frac{E_m h^3}{q_0 L^4} w \left(\frac{L}{2} \right) \quad (10) \quad \bar{\sigma}_x = \frac{h}{q_0 L} \sigma_x \left(\frac{L}{2}, \frac{h}{2} \right) \quad (11)$$

$$\bar{\tau}_{xz} = \frac{h}{q_0 L} \tau_{xz} (0,0) \quad (12) \quad \bar{\omega} = \frac{\omega L^2}{h} \sqrt{\frac{\rho_m}{E_m}} \quad (13)$$

Table 2 presents the deflection results corresponding to uniform and sinusoid loads for different L/h and p . The deflection increases with increasing p and decreases with increasing L/h . For the sinusoidal loading case, the deflection is found to be lower compared to the one of the uniform load cases. Table 3 demonstrates the results of displacement and stresses induced in an FG beam for various theories. The displacements are less for uniform load than the ones for sinusoidal load. Except for the classical beam theory, all other theories give similar results.

Table 2: Non-dimensional deflection of functionally graded (P-FGM) beams (Voigt model)

L/h	p	Theory	Uniform load	Sinusoidal load	
5	0	(Sayyad & Ghugal, 2018)	3.1635	2.5004	
		Present study	3.1654	2.5019	
	1	(Sayyad & Ghugal, 2018)	6.2563	4.9432	
		Present study	6.2594	4.9457	
	2	(Sayyad & Ghugal, 2018)	8.0666	6.3745	
		Present study	8.0677	6.3754	
	5	(Sayyad & Ghugal, 2018)	9.8414	7.7830	
		Present study	9.8281	7.7723	
	10	(Sayyad & Ghugal, 2018)	10.940	8.6547	
		Present study	10.9381	8.6530	
	10	0	(Sayyad & Ghugal, 2018)	2.9496	2.3271
			Present study	2.9501	2.3275
1		(Sayyad & Ghugal, 2018)	5.8951	4.6506	
		Present study	5.8959	4.6512	
2		(Sayyad & Ghugal, 2018)	7.5671	5.9698	
		Present study	7.5673	5.9699	
5		(Sayyad & Ghugal, 2018)	9.0238	7.1207	
		Present study	9.0204	7.1179	
10		(Sayyad & Ghugal, 2018)	9.9411	7.8452	
		Present study	9.9403	7.8446	

Table 3: Non-dimensional displacements and stresses of P-FGM beams (Voigt model, $L = 5h$)

p	Theory	Model	Uniform load			Sinusoidal load		
			\bar{w}	$\bar{\sigma}_x$	$\bar{\tau}_{xz}$	\bar{w}	$\bar{\sigma}_x$	$\bar{\tau}_{xz}$
0	Present	RBT	3.1654	3.8019	0.7329	2.5020	3.0916	0.4769
	(Sayyad & Ghugal, 2018)	ESDBT	3.1635	3.8084	0.7764	2.5004	3.0979	0.5072
	(Reddy, 1984)	HSDBT	3.1654	3.8028	0.7305	2.5020	3.0916	0.4769
	(Timoshenko, 1921)	FSDBT	3.1657	3.7501	0.4922	2.5023	3.0396	0.3183
	(Euler, 1744)	CBT	2.8783	3.7501	–	2.2693	3.0396	–
1	Present	RBT	6.2594	5.8835	0.7329	4.9458	4.7856	0.4769
	(Sayyad & Ghugal, 2018)	ESDBT	6.2563	5.8957	0.8288	4.9432	4.7964	0.5430
	(Reddy, 1984)	HSDBT	6.2594	5.8850	0.8031	4.9458	4.7856	0.5243
	(Timoshenko, 1921)	FSDBT	6.1790	5.7960	0.8313	4.8807	4.6979	0.3183
	(Euler, 1744)	CBT	5.7746	5.7960	–	4.5528	4.6979	–
2	Present	RBT	8.0677	6.8824	0.6704	6.3754	5.6004	0.4368
	(Sayyad & Ghugal, 2018)	ESDBT	8.0666	6.8971	0.8485	6.3745	5.6149	0.5553
	(Reddy, 1984)	HSDBT	8.0677	6.8842	0.8446	6.3754	5.6004	0.5521
	(Timoshenko, 1921)	FSDBT	7.9253	6.7678	1.0791	6.2601	5.4856	0.2709
	(Euler, 1744)	CBT	7.4003	6.7678	–	5.8346	5.4856	–
5	Present	RBT	9.8281	8.1104	0.5904	7.7723	6.6057	0.3856
	(Sayyad & Ghugal, 2018)	ESDBT	9.8414	8.1331	0.7654	7.7830	6.6281	0.5024
	(Reddy, 1984)	HSDBT	9.8281	8.1127	0.8114	7.7723	6.6057	0.5314
	(Timoshenko, 1921)	FSDBT	9.4987	7.9430	1.5373	7.5056	6.4382	0.2085
	(Euler, 1744)	CBT	8.7508	7.9430	–	6.8994	6.4382	–
10	Present	RBT	10.9381	9.7119	0.6465	8.6530	7.9080	0.4224
	(Sayyad & Ghugal, 2018)	ESDBT	10.940	9.7345	0.6947	8.6547	7.9300	0.4560
	(Reddy, 1984)	HSDBT	10.938	9.7141	0.6448	8.6530	7.9080	0.4224
	(Timoshenko, 1921)	FSDBT	10.534	9.5231	1.9050	8.3259	7.7189	1.2320
	(Euler, 1744)	CBT	9.6072	9.5231	–	7.5746	7.7189	–

Table 4 presents the non-dimensional natural frequency of P-FGM beams of various theories for varying p . It can be seen that the present methodology shows good agreement with results from the published literature. The natural frequency decreases as p increases.

Table 4: Non-dimensional flexural natural frequencies ($\bar{\omega}$) of simply supported P-FGM beams (Voigt model)

L/h	Mode	Theory	Model	Power law index (p)					
				0 (ceramic)	1	2	5	10	∞ (Metal)
5	1	Present	RBT	5.15274	3.99042	3.62643	3.40120	3.28160	2.67732
		(Sayyad & Ghugal, 2018)	ESDBT	5.15423	3.99140	3.62671	3.40000	3.28135	2.67810
		(Reddy, 1984)	HSDBT	5.15274	3.99042	3.62643	3.40120	3.28160	2.67732
		(Şimşek, 2010)	FSDBT	5.15247	3.99023	3.63438	3.43119	3.31343	2.67718
		(Şimşek, 2010)	HSDBT	5.15274	3.99042	3.62643	3.40120	3.28160	2.67732
		(Thai & Vo, 2012)	HSDBT	5.15275	3.99042	3.62644	3.40120	3.28160	2.67732
		(Vo et al., 2014)	FSDBT	5.15260	3.97108	3.60495	3.40253	3.29625	2.67725
		(Vo et al., 2014)	HSDBT	5.15275	3.97160	3.59791	3.37429	3.26534	2.67732
		(Timoshenko, 1921)	FSDBT	5.15247	3.99023	3.63438	3.43119	3.31343	2.67718
		(Euler, 1744)	CBT	5.39530	4.14840	3.77930	3.59490	3.49210	2.80336
20	1	Present	RBT	5.46032	4.20505	3.83613	3.64849	3.53898	2.83714
		(Sayyad & Ghugal, 2018)	ESDBT	5.46043	4.20513	3.83614	3.64830	3.53895	2.83720
		(Reddy, 1984)	HSDBT	5.46030	4.20503	3.83611	3.64850	3.53896	2.83716
		(Şimşek, 2010)	FSDBT	5.46032	4.20505	3.83676	3.65088	3.54156	2.83713
		(Şimşek, 2010)	HSDBT	5.46030	4.20503	3.83611	3.64850	3.53896	2.83716
		(Thai & Vo, 2012)	HSDBT	5.46032	4.20505	3.83613	3.64849	3.53899	2.83714
		(Vo et al., 2014)	FSDBT	5.46033	4.20387	3.83491	3.64903	3.54045	2.83714
		(Vo et al., 2014)	HSDBT	5.46032	4.20387	3.83428	3.64663	3.53787	2.83714
		(Timoshenko, 1921)	FSDBT	5.46032	4.20505	3.83676	3.65088	3.54156	2.83713
		(Euler, 1744)	CBT	5.47770	4.21630	3.84720	3.66280	3.55470	2.84618

Table 5 presents the displacement and stress results at different loads, namely under uniform and sinusoidal, for different material models. The difference in the results is because each case estimates the properties using different material models. The displacement is minimum for the Voigt and maximum for the Reuss model because these models are the ideal models and are best applicable for long fibers in which the bonding is perfect. Naturally, the results of the other models such as LRVE, Tamura, and Mori-Tanaka fall inside these upper and lower bands formed by the Reuss and Voigt models. The rule of mixture could not predict the properties of particle composite effectively, but it can be applied for lower ratios of material combinations. Its applicability can be extended in modeling the porosity effects, as well. The magnitude of results is found to be lower for the sinusoidal load and higher for the uniform load.

Table 5: Non-dimensional displacements and stresses of P-FGM beams ($p=2$ and $L = 5h$)

		Uniform load			Sinusoidal load		
Theory (Model)		\bar{w}	$\bar{\sigma}_x$	$\bar{\tau}_{xz}$	\bar{w}	$\bar{\sigma}_x$	$\bar{\tau}_{xz}$
Present	Voigt (Voigt, 1889)	8.0677	6.8824	6.3754	2.4047	5.6004	0.4368

Reuss (Reuss, 1929)	10.1403	8.9372	8.0184	2.8647	7.2756	0.4231
LRVE (Gasik, 1998)	9.3292	7.8585	7.3756	2.7326	6.3981	0.4104
Tamura (Nakamura et al., 2000)	10.1403	8.9372	8.0184	2.8647	7.2756	0.4231
(q=0)	9.2981	7.9333	7.3504	2.7089	6.4583	0.4184
(q=100)						
Mori-Tanaka (Tanaka et al., 1993)	9.8633	8.5824	7.7989	2.8166	6.9869	0.4206

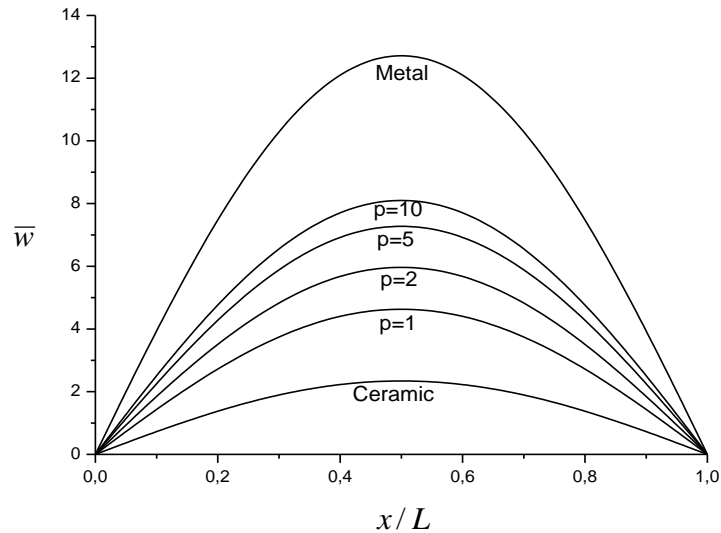


Fig. 4: The variation of the transverse displacement \bar{w} for L/h

Fig. 4 shows the variation of displacement along x/L . The displacement is maximum for the pure metal case ($p=\infty$), and it decreases with decreasing p and reaches its minimum for the pure ceramic case ($p=0$) because ceramics have higher modulus of elasticity compared to metal.

Finally, Table 6 presents the natural frequency results for the cases $L/h=5$ and $L/h=20$. The frequency is maximum when there is no porosity present and decreases as the porosity fraction increases. Three different types of porosity variations were considered, namely the even case (Imperfect-1), the uneven case (Imperfect-2), and the logarithmic-uneven (Imperfect-3). The analysis shows that the Imperfect-1 case has the lowest frequency; the maximum is achieved for Imperfect-3, while Imperfect-2 gives intermediate results. The results of Imperfect-2 and Imperfect-3 yield quite similar results. As the natural frequencies obtained for Imperfect-2 and Imperfect-3 are similar, a fabrication process that leads to uneven porosity distribution can be selected.

Table 6: Variation of frequency parameters $\bar{\omega}$ of perfect and imperfect FG beam ($p=2$)

L/h	Perfect	Imperfect I (even)		Imperfect II (uneven)		Imperfect III (Logarithmic-uneven)	
	$a = 0$	$a = 0.1$	$a = 0.2$	$a = 0.1$	$a = 0.2$	$a = 0.1$	$a = 0.2$
5	3.6264	3.4418	3.1489	3.6069	3.5785	3.6075	3.5816
20	3.8361	3.6335	3.3123	3.8226	3.8004	3.8230	3.8029

5 Conclusion

The conclusion of the research work can be summarized in the following points:

1. If the distribution of porosity in the beam is of imperfect type-1 (even) then the natural frequency would be minimum. The natural frequency is maximum for the case of imperfect type-3 (logarithmic-uneven). Therefore, a manufacturing technique would be intended to get a porosity development of logarithmic type and not evenly distributed. As expected, the natural frequency decreases with the introduction of porosity because of the degradation of material properties.
2. The dimensionless transverse displacement is minimum for ceramic and maximum for metal and intermediate in the case of FGMs, so a beam which is ceramic rich ($p=0$) yields lower displacements compared to a beam which is metal-rich ($p=10$) in composition.
3. The Voigt model gives the lowest displacement and the Reuss model gives the maximum. The Tamura model and Reuss gave identical results. The results of the present method show good agreement with the ones of the other theories published in the literature.

References

- Avcar, M. (2019). "Free vibration of imperfect sigmoid and power law functionally graded beams." *Steel and Composite Structures*, 30(6), 603-615. DOI: <https://doi.org/10.12989/scs.2019.30.6.603>.
- Benaberrahmane, I. et al. (2021). "Investigating of free vibration behavior of bidirectional FG beams resting on variable elastic foundation." *Geomechanics and Engineering*, 25(5), 383-394. DOI: <https://doi.org/10.12989/gae.2021.25.5.383>.
- Euler, L. (1744). *Methodus inveniendi lineas curvas maximi minimive proprietate gaudentes, sive solutio problematis isoperimetrici lattissimo sensu accepti*, apud Marcum-Michaelem Bousquet & Socios, Lausannae & Genevae.
- Gasik, M. M. (1998). "Micromechanical modelling of functionally graded materials." *Computational Materials Science*, 13(1), 42-55. DOI: [https://doi.org/10.1016/S0927-0256\(98\)00044-5](https://doi.org/10.1016/S0927-0256(98)00044-5).
- Hadji, L. & Avcar, M. (2021). "Free Vibration Analysis of FG Porous Sandwich Plates under Various Boundary Conditions ".*Journal of Applied and Computational Mechanics*, 7(2), 505-519. DOI: <https://doi.org/10.22055/jacm.2020.35328.2628>.
- Larbi, L. O. et al. (2013). "An Efficient Shear Deformation Beam Theory Based on Neutral Surface Position for Bending and Free Vibration of Functionally Graded Beams#." *Mechanics Based Design of Structures and Machines*, 41(4), 421-433. DOI: <https://doi.org/10.1080/15397734.2013.763713>.
- Madan, R. & Bhowmick, S. (2021). "A numerical solution to thermo-mechanical behavior of temperature dependent rotating functionally graded annulus disks." *Aircraft Engineering and Aerospace Technology*, 93(4), 733-744. DOI: <https://doi.org/10.1108/AEAT-01-2021-0012>.
- _____. (2022). "Modeling of functionally graded materials to estimate effective thermo-mechanical properties." *World Journal of Engineering*, 19(3), 291-301. DOI: <https://doi.org/10.1108/WJE-09-2020-0445>.
- Nakamura, T., Wang, T. & Sampath, S. (2000). "Determination of properties of graded materials by inverse analysis and instrumented indentation." *Acta Materialia*, 48(17), 4293-4306. DOI: [https://doi.org/10.1016/S1359-6454\(00\)00217-2](https://doi.org/10.1016/S1359-6454(00)00217-2).
- Nguyen, D. K. et al. (2017). "Vibration of bi-dimensional functionally graded Timoshenko beams excited by a moving load." *Acta Mechanica*, 228(1), 141-155. DOI: <https://doi.org/10.1007/s00707-016-1705-3>.
- Plevris, V. & Tsiatas, G. (2018). "Computational Structural Engineering: Past Achievements and Future Challenges." *Frontiers in Built Environment*, 4(21), 1-5. DOI: <https://doi.org/10.3389/fbuil.2018.00021>.
- Reddy, J. N. (1984). "A Simple Higher-Order Theory for Laminated Composite Plates." *Journal of Applied Mechanics*, 51(4), 745-752. DOI: <https://doi.org/10.1115/1.3167719>.

- Reuss, A. (1929). "Berechnung der Fließgrenze von Mischkristallen auf Grund der Plastizitätsbedingung für Einkristalle." *ZAMM - Journal of Applied Mathematics and Mechanics / Zeitschrift für Angewandte Mathematik und Mechanik*, 9(1), 49-58. DOI: <https://doi.org/10.1002/zamm.19290090104>.
- Sankar, B. V. (2001). "An elasticity solution for functionally graded beams." *Composites Science and Technology*, 61(5), 689-696. DOI: [https://doi.org/10.1016/S0266-3538\(01\)00007-0](https://doi.org/10.1016/S0266-3538(01)00007-0).
- Sayyad, A. S. & Ghugal, Y. M. (2018). "An inverse hyperbolic theory for FG beams resting on Winkler-Pasternak elastic foundation." *Advances in aircraft and spacecraft science*, 5(6), 671-689. DOI: <https://doi.org/10.12989/aas.2018.5.6.671>.
- Şimşek, M. (2010). "Fundamental frequency analysis of functionally graded beams by using different higher-order beam theories." *Nuclear Engineering and Design*, 240(4), 697-705. DOI: <https://doi.org/10.1016/j.nucengdes.2009.12.013>.
- Tanaka, K. et al. (1993). "An improved solution to thermoelastic material design in functionally gradient materials: Scheme to reduce thermal stresses." *Comput. Methods Appl. Mech. Engrg.*, 109(3), 377-389. DOI: [https://doi.org/10.1016/0045-7825\(93\)90088-F](https://doi.org/10.1016/0045-7825(93)90088-F).
- Thai, H. T. & Vo, T. P. (2012). "Bending and free vibration of functionally graded beams using various higher-order shear deformation beam theories." *International Journal of Mechanical Sciences*, 62(1), 57-66. DOI: <https://doi.org/10.1016/j.ijmecsci.2012.05.014>.
- Timoshenko, S. P. (1921). "LXVI. On the correction for shear of the differential equation for transverse vibrations of prismatic bars." *The London, Edinburgh, and Dublin Philosophical Magazine and Journal of Science*, 41(245), 744-746. DOI: <https://doi.org/10.1080/14786442108636264>.
- Vo, T. P., Thai, H.-T., Nguyen, T.-K., Maheri, A., and Lee, J. (2014). "Finite element model for vibration and buckling of functionally graded sandwich beams based on a refined shear deformation theory." *Eng. Struct.*, 64, 12-22. DOI: <https://doi.org/10.1016/j.engstruct.2014.01.029>.
- Voigt, W. (1889). "Ueber die Beziehung zwischen den beiden Elasticitätsconstanten isotroper Körper." *Annalen der Physik*, 274(12), 573-587. DOI: <https://doi.org/10.1002/andp.18892741206>.

Cite as: Hadji L., Plevris V. & Madan R., "A Static and Free Vibration Analysis of Porous Functionally Graded Beams", *The 2nd International Conference on Civil Infrastructure and Construction (CIC 2023)*, Doha, Qatar, 5-8 February 2023, DOI: <https://doi.org/10.29117/cic.2023.0059>